THE JOURNAL OF PHYSICAL CHEMISTRY B

ARTICLE

pubs.acs.org/JPCB

Interfacial Viscoelasticity of Myoglobin at Air/Water and Air/Solution Interfaces: Role of Folding and Clustering

Kamatchi Sankaranarayanan,[†] Aruna Dhathathreyan,[*,†] Jürgen Krägel,[‡] and Reinhard Miller[‡]

[†]Chemical Lab., CSIR-CLRI, Adyar, Chennai 600020, India

[‡]MPI für Kolloid- und Grenzflächenforschung, Wissenschaftspark Golm, D-14424 Golm, Germany

ABSTRACT: This study describes the folding and organization of myoglobin (Mb) at the solution/air interface at different pH values of 2.5, 3.5, 5.5, 7.5, and 8.5. Dynamic surface tension and the associated dilational and shear viscoelasticity for Mb at these pH's have been studied using a sinusoidal surface compression and expansion for frequencies ranging from 0.01 to 0.4 Hz. The changes in dilational viscosity, elasticity, and fluorescence lifetime measurements have been related to the conformational changes of the protein films at the interface. It is observed that while acid-induced denaturation of the protein does not lead to large changes in dilational properties, the shear properties on the other hand are strongly influenced by it, and the protein behaves like a shear-thickening fluid. At higher pH, particularly at the isoelectric point, Mb is pseudoplastic indicating an increase in the shear viscosity. These results are strongly suggestive of formation of hydrophobic clusters at the protein−buffer interface because of the change in the overall charge distributions.

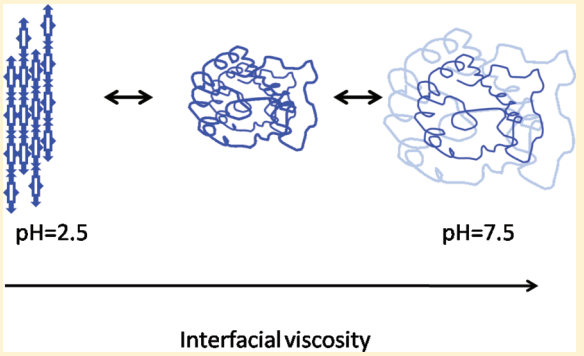

INTRODUCTION

The process of protein folding is an inherently complex process along an energy landscape that involves segmental motions of the protein along with interactions with surrounding solvent molecules.[1] The viscosity of solvent directly affects protein conformational transitions. On the other hand, cellular biomechanics primarily determined by viscoelastic properties of the cytoplasm and the cell membrane change in various states of disease.[2,3] The miracle of any of these protein structures and functions is that the global stability (the free-energy difference between the folded and the unfolded state) at room temperature is about 20 k_bT or about 10 kcal/mol for a 100 residue domain. Failure to fold into the intended shape usually produces inactive proteins with different properties.

Several research groups have studied the interactions that contribute to the stability of proteins.[4−12] Miller et al. have recently in a comprehensive review enumerated the importance of rheological parameters in understanding interfacial processes.[13] Dilational and shear rheological properties of adsorbed layers of milk protein beta-casein (BCS) mixed with the charged and neutral surfactants have been experimentally studied, and theoretical models to understand the diffusion to the interface in these binary systems have been developed.[14] Viscoelasticity of mixed adsorption layers from the adsorption characteristics of the single components has been evaluated for human serum albumin and surfactant mixtures using dilational elasticity and viscosity of surface layer.[15] Lakshmanan et al. and Muthuselvi et al. have studied different interfacial properties of proteins in the presence of additives and have observed anomalous viscoelastic behavior in these systems.[16,17] Using dilational rheology and adsorption studies with quartz crystal microbalance (QCM), Muthuselvi et al. have shown that any proposed denaturation mechanism of large biomolecules requires very high concentrations of urea and that the association of urea with protein−water system is based on enhancement of hydrophobic interactions.[17]

Recently, there has been a concerted effort to determine the structures of the denatured state ensemble (DSE)[18] whose experimental resolution is difficult because of fluctuations in the unfolded structures. In particular, it is difficult to determine the properties of the DSE under conditions in which the native state is stable because the population of the unfolded structures is low.[19]

Denaturants, such as urea and guanidinium chloride (GdmCl), destabilize proteins. In contrast, osmolytes that protect cells against environmental stresses such as high temperature, desiccation, and pressure can stabilize proteins.[20]

One of the important issues that is being addressed is how perturbations occurring at a local site in the biomolecule because of different solvation of specific functional groups/side chains of the amino acids in specific domains impart a conformational change at a distant spot lying several nanometers away.[21−23]

Thus, a complete understanding of the stability of proteins and a description of the structures in the diverse DSEs require experimental and theoretical studies that provide a quantitative

Received: October 20, 2011
Revised: December 9, 2011
Published: December 18, 2011

description of the effects of both osmolytes and denaturants. O'Brien et al. have used the molecular transfer model to show that the presence of denaturants and osmolytes affects the denatured state ensemble.[24] Sharma et al. have described a simple additive model to extract interfacial viscosity contribution from bulk viscosity measurements for different shear rates and have applied it to bovine serum albumin (BSA).[25] Stokes and Frith have in a recent work correlated the mechanical response with the microstructure of structured soft matter in the context of flow behavior of these materials.[26] Dimitrijev-Dwyer and Middelberg have used a generalized Maxwell model for beta-lactoglobulin, lysozyme, BSA, and beta casein and have demonstrated that viscoelastic relaxations occur on multiple time scales which ultimately determine the interfacial rheology and its dependence to mass transfer from bulk.[27]

Ermi has recently published an elegant review on deformation modes of complex fluid interfaces where he has highlighted the relation between interfacial rheology, interface structure, and macroscopic material properties of complex fluids and their role in the context of adsorption layers formed by surfactants, proteins, and nanoparticles and for composite interface.[28] Noskov et al. have in a recent work demonstrated the impact of global unfolding on dilational viscoelasticity of β-lactoglobulin adsorbed layers.[29]

Several research papers have appeared in the literature on the interaction of redox proteins like hemoglobin, myoglobin, and cytochrome C which have addressed the above issues and have created models on the basis of either experimental studies or molecular dynamics simulations (MDS).[30−32] Mb like all heme proteins can initiate lipid oxidation, and its own oxidation is highly pH dependent. Park and Park[33] have extracted Mb from Pacific sardine and have added to Pacific whiting surimi to measure its effects on protein gelation. Gunda and Mitra[34] have developed a mathematical model for simulating the dielectrophoretic behavior of a Mb molecule in a microchannel in connection with purification and separation of the protein.

Important vibrational energy relaxations involved in the heme group in Mb in different solvent environments have been studied using MDS by Zhang et al.[35] Mb in various disaccharide−water environments has been examined at different temperatures, and its denaturation behavior has been related to the glass-transition temperature of the solvent systems.[36] The dynamic heterogeneity in the protein dynamics arising from the different relaxation mechanisms of the solvent occurring at different rates has been studied for Mb using infrared vibrational echo experiments. The results show clearly that Mb adopts multiple, slowly interchanging conformational substates, and these conformations transmit to surface changes that result in heterogeneous dynamics.[37] Variable temperature studies on secondary structural changes in Mb in the presence of sodium dodecyl sulfate (SDS) have been reported.[38]

Mb is an important cardiac marker whose concentration increases drastically in the blood serum of human beings after a minor heart attack. Quantifying the Mb after detection is important for development of a diagnostic tool. Finkelstein et al. used spectrally resolved stimulated vibrational echo spectroscopy to investigate the dependence of fast protein dynamics on bulk solution viscosity at room temperature in three heme proteins: hemoglobin, myoglobin, and a myoglobin mutant. The viscosity-dependent protein dynamics are analyzed in the context of a viscoelastic relaxation model that treats the protein as a deformable breathing sphere.[39]

In recent times, studies on proteins in solutions have shown that it is possible to increase protein stability by improving electrostatic interactions among charged groups on the surface of the folded protein. An analysis of stabilization of different folded states of the proteins in various solvents suggests that even when the hydrophobic and hydrogen-bonding interactions that stabilize the folded state are disrupted, charge−charge interactions on the exposed residues can reduce the net electrostatic interactions and can even determine the stability of the denatured state ensemble. In this context, because of the asymmetry that exists at the air/water interface, changes in hydrophobic and H-bonding interactions and the intermediate folding states of the protein at the interface offer a good starting point to study the factors that contribute to the stability of the protein and to model the denatured state ensembles.[40]

In the present work, the effect of pH on the rheological behavior of Mb at air/solution interface has been studied using both dilational and interfacial shear rheology. The changes occurring at the interface at different pH's have been characterized using circular dichroism (CD) spectroscopy and time-resolved fluorescence emission. The surface charges in the protein have been related to interface structure and macroscopic material properties.

EXPERIMENTAL SECTION

Materials. Horse heart myoglobin was purchased from Biozyme (Reinheitszahl 1/4 4.8) (San Diego, CA) and was used without further purification. Before each experiment, the protein was dissolved in 20 mM 4-morpholinepropanesulfonic acid (Boehringer Mannheim, Ingelheim am Rhein, Germany) at pH 7.0 and was filtered with Millipore (Billerica, MA) Millex SV filters before use. Concentration of Mb solution was fixed at 10^{-6} M for all pH values. Glycine-HCl buffer was used for preparation of Mb solution at pH = 2.5. Phosphate buffer (100 mM) was used to prepare protein solutions pH 5.5, 7.5, and 8.5.

To Mb, in the respective buffer were added a few crystals of sodium dithionite (final concentration 0.2 mg/mL) to ensure that the oxygen was removed after storing a gastight sample container. The excess of dithionite was eliminated by gel filtration chromatography on a column (20 cm × 1.5 cm) filled with Sephadex G-25 (Pharmacia, Sweden).

Methods. *Surface and Interfacial Properties of Mb at Different pH's.* Freshly prepared solutions of the protein at the different pH's were used for each measurement. Equilibrium surface tension values as a function of time were first measured using an NIMA DST 9005 tensiometer fitted with a Wilhelmy plate (CHR1 chromatography paper). A Teflon trough of capacity 30 mL was used, and for every measurement, the protein solution at the prescribed pH was poured and the Wilhelmy plate was dipped to a designated fixed height. The surface was swept before each measurement ensuring that no aggregates of the protein were present at the surface at time t = 0. The dilational rheological parameters of the solutions at pH 2.5, 3.5, 5.5, 7.5, and 8.5 were measured with the profile analysis tensiometer PAT-1 (SINTERFACE Technologies, Germany) with an accuracy of ±0.1 mN/m and were thermostated at a temperature of 22 °C. The solution drops were formed at the tip of a PTFE capillary immersed into a cuvette filled with a water-saturated atmosphere. After having reached the adsorption equilibrium, the solution drop was subjected to harmonic oscillations with frequencies (f) 0.01−0.2 Hz in order to study the dilatational

elasticity.[41] Accuracy in elasticity and viscosity values are ±1 mN/m and ±1 mNs/m. Each measurement was repeated at least three times, and the averages of these three measurements are presented in this study. The surface tension oscillations were measured parallelly. The elasticity modulus was determined from the amplitude ratio of the oscillations of surface tension and surface area. To correlate the degree of elasticity of the protein molecules covering the surface, a correlation between the surface tension and the change in elasticity for different frequencies has been carried out using a biexponential fit using the equation of the form

$$Y = y_0 + A_1 e^{-x/t1} + A_2 e^{-x/t2} \quad (1)$$

where t_1 and t_2 are the time constants and A's are the amplitudes. Here, the value of y_0 is the offset which can be related to the threshold surface coverage that is required for the system to be elastic.

In a separate experiment, the protein films were spread in a Langmuir trough fitted with a Wilhelmy plate. The simplest common method of studying the compression modulus is to perform oscillatory compressions of the film with the Langmuir trough barriers measuring the surface pressure and the phase shift between the surface tension signal and the surface area. By carrying out such uniaxial compressions, the film is actually subject to both compression and shear. The effect of shear modulus can be overlooked assuming that it is negligible compared to the compression modulus. Following a method developed by Cicuta and Terentjev,[42] spread monolayers of Mb (from very low dilutions) in a Langmuir trough were compressed using two symmetrical barriers and two Wilhelmy balances positioned at midway; the films were compressed at about 5 cm^2/min. The surface pressure was recorded as a function of time, while the area was changed by imposed oscillatory barrier movements. The surface pressure was measured with the two Wilhelmy plates at orthogonal orientations. In every experiment, the films were subjected to a 20 oscillation cycle and then were aged for about 1 to 2 h. After equilibrium values were reached, the protein films from the surface were then skimmed and characterized using fluorescence and circular dichroism spectroscopy.

Picosecond-Time-Resolved Fluorescence Spectroscopy. Fluorescence lifetime measurements of samples have been carried out in a picosecond-time-correlated single-photon-counting (TCSPC) spectrometer. The excitation source is the tunable Ti−sapphire laser (Spectra Physics, United States). The laser pulse (pulse width of 2 ps and repetition rate of 4 MHz) has been derived from the frequency-doubled output (532 nm) of mode-locked laser (Spectra Physics, United States). The picosecond standard tuning range is 720−850 nm. The sample was excited by the laser pulse at 280 nm, and emission was monitored at right angles to the excitation path. The first photon was detected by the micro channel plate photomultiplier tube (MCP-PMT) (Hamamatsu-C 4878). When the first excitation pulse occurred, a synchronization pulse triggered the charging of the capacitor in the time to amplitude convertor (TAC) through the discriminator. The voltage on the capacitor increased linearly until a stop timing pulse was detected on repeating the start−stop cycle, and a histogram representative of the fluorescence decay was obtained which has been further analyzed using the IBH (Glasgow, United Kingdom) software.[43]

Circular Dichroic Spectroscopy. Circular dichroism measurements were performed on samples of Mb using a spectropolarimeter, model J-710 (Jasco, Japan), equipped with a Neslab RTE-110 temperature controller (Neslab Instruments, United States) and calibrated with a standard solution of (+)-10-camphorsulfonic acid. Cuvettes of 0.1 cm path length (Hellma, United States) were used in the far-UV (190−240 nm), and cuvettes of 1.0 cm path length were used in the near-UV (250−330 nm). Photomultiplier voltage did not exceed 600 V in the spectral regions measured. Each spectrum was signal-averaged at least five times; was smoothed with Spectropolarimeter System Software, version 1.00 (Jasco); and was baseline-corrected by subtracting the buffer spectrum. All the measurements were performed at 30 °C under a nitrogen flow (3 L/h). The secondary structural features were fitted using Dichroweb.[44]

Surface-Shear Measurements and Calculation of Rheological Parameters. The surface-shear rheology was measured with the torsion pendulum rheometer described elsewhere in detail.[45] The instrument used in this study was the torsion pendulum rheometer (interfacial shear rheometer ISR-1, SINTERFACE Technologies, Germany). Briefly described, the rheometer makes a small deflection (0.5−3°) of the measuring body, which is a sharp-edged ring with a hydrophobic titanium surface, suspending on a 100 μm diameter tungsten torsion wire.

Similar to the surface tension measurements, the protein solution at the defined pH was poured into the Teflon vessel. The solution surface was cleaned by suction immediately before the experiment to remove any surface impurities or air bubbles. Then, the solution surface was touched with the sharp edge of the measuring body. When the system has reached mechanical equilibrium, the program automatically starts the measurement.

The oscillation frequency of the torsion pendulum is 0.1 Hz. Using this device, interfacial shear elasticities and viscosities as a function of adsorption time in steps of 5−10 min can be determined in the range of 10^{-6} to 10^{-3} Nm^{-1} and 10^{-5} to 10^{-2} Nsm^{-1}, respectively. All rheological experiments were performed with a deflection angle of 2° so as to minimize disruption of the interfacial layers. The measuring geometry yields an initial relative deformation of the surface of 8.7%. The pendulum experiments which last each approximately 30 s were repeated every 10 min over a period of 4 h. The bulk viscosity values for the protein samples at the different pH's were measured using a quartz crystal microbalance (Maxtek model RQCM) and a gold-coated AT cut quartz operating at 5 MHz.

RESULTS AND DISCUSSION

At very low Mb concentrations used in the present study, it is expected that no aggregation or intermolecular interactions interfere with the measurements of dilational moduli which should lead to an optimal assembly process at air/solution interface. For every pH solution used, after about 16 000 s, the adsorption equilibrium was achieved, and harmonic oscillations of the drop area with a magnitude of change in drop surface area $\Delta\Omega$ (7−8%) and frequencies in the range between 0.01 and 0.4 Hz were generated. Figure 1a illustrates the experimental change in surface pressure ($\gamma_{H20} - \gamma_{H2O+Mb}$) of Mb at the different pH values of 2.5, 3.5, 5.5, 7.5, and 8.5 as a function of time adsorbed at solution/air interface. All the measurements were made after ensuring that water evaporation does not take place, and the reference surface tension value of the subphase was maintained constant before each measurement. The diffusion of Mb from the bulk to the surface regulates the adsorption kinetics initially after which any further change in the surface pressure can

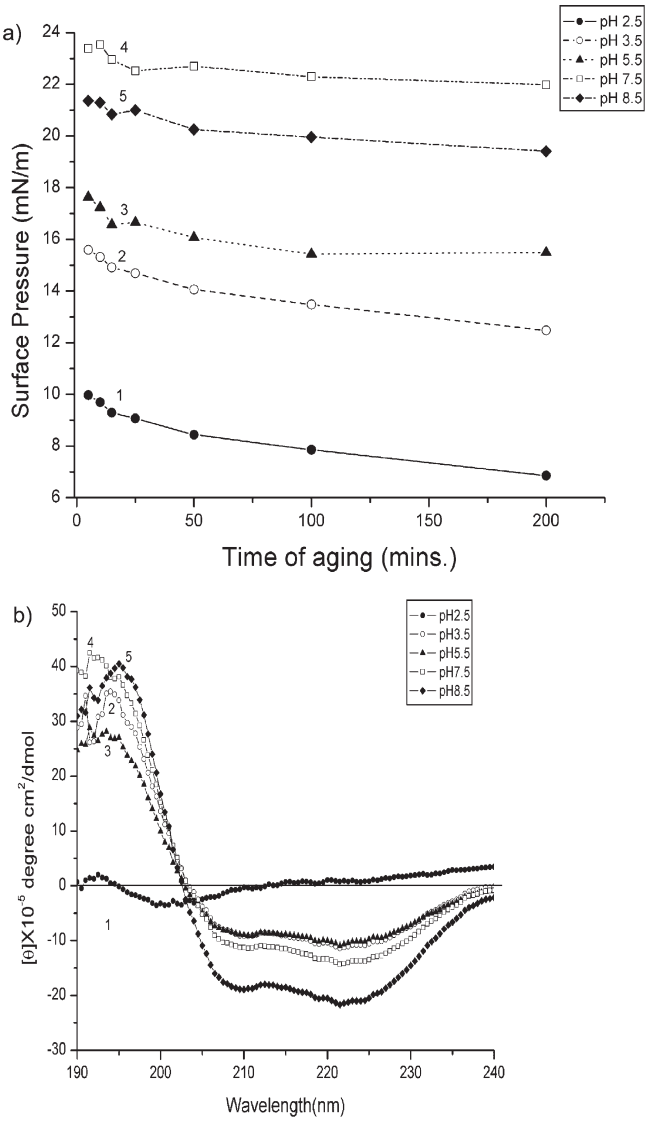

Figure 1. (a) Change in surface pressure of Mb solution at different pH values of 2.5, 3.5, 5.5, 7.5, and 8.5. (b) CD spectra of protein (skimmed from air/solution interface after equilibrium) at different pH values.

be associated with reorganization of the protein and new interaction between the segments at the solution/air interface.

The plots show that the surface activity of Mb is highest at pH 7.5 which is the isoelectric point of the protein. The surface activity decreases with time for all pH's. The surface dilational rheology involves compression and expansion cycles of the surface layer that disturbs the prevailing equilibrium. As a result of this, the protein molecules must remain dissolved in the bulk or must adsorb at the interface to restore the equilibrium coverage. In this regard, the time frame of the internal relaxation processes is an important factor that determines the overall conformation of the protein at the interface and the ability of these molecules to optimize the surface coverage and to reach maximum surface activity. Thus, the surface pressure or change in surface tension is a measure of the resistance against area changes and the ability of the surface to re-establish equilibrium. In the present study, surface pressure shows maximum value at pI (7.5) which suggests that in addition to better surface coverage by Mb molecules, the molecular exchange between the bulk and the

Table 1. Secondary Structural Features of Mb at Different pH's

Mb/pH	% H(r)	% H(d)	% S(r)	% S(d)	% turn	% unrd
2.5	0.4	3.8	34.5	12.8	9.6	38.9
3.5	75.8	17.2	1.4	0	0	5.6
5.5	73.4	22.9	0.7	0	0	3.1
7.5	84.4	14	1.4	0	0	0.2
8.5	74.6	25.4	0	0	0	0

interface is suppressed. On the basis of the change in the surface pressure over time, the adsorption layer can be likened to an insoluble monolayer.

Figure 1b shows the CD spectra of Mb after being subjected to oscillations and after aging in the Langmuir trough at different pH's. It is seen that at pH = 2.5 the secondary structural features show a large percentage of β sheet compared with all other pH values. At pI, the CD spectra show maximum helicity, and the corresponding secondary structural features of Mb are given in Table 1. From the table, it is seen clearly that at the lowest pH the protein has a large % of β sheet and also nearly 39% of unordered structure. As pH is increased, the % helicity increases, and at pI, it shows a maximum helicity of 98.4%.

The above samples used for the rheological studies were subjected to time-resolved fluorescence emission intensity decay of Mb at the different pH values, and the lifetimes of the decay were assigned for the different samples.

Figure 2 shows the fluorescence decay plots of Mb at different pH values. Table 2 shows the decay times of Mb in different buffer solutions. It has been observed that fluorescence lifetimes of different tryptophan residues in heme proteins generally lie in the picosecond range because of very efficient electron transfer from the excited state of tryptophan to the heme.[46,47] In an earlier study, the shorter lifetimes have been assigned to the Trp7 and Trp14 residues in the presence of normal hemes. The τ_2 has been assigned to Trp7 with inverted hemes while τ_3 has been assigned to reversibly heme dissociated Mb.[48] At pH 2.5, the decay profile is biphasic with the amplitudes being nearly equal for τ_1 and τ_2.

Comparing the CD spectral studies with the fluorescence decays at pH 2.5, the τ_1 and τ_2 may be assigned to the ordered and disordered heme populations arising through the secondary structural features. At all other pH values, the decay profile is triphasic with the maximum population showing a decay time of 0.19 ns. The decay profiles of 1.5 and 4.4 ns show a narrow population distribution which indicates a rigid homogeneous Mb structure. It is necessary to differentiate whether the changes in the lifetimes and the populations are due to the changes in the geometries of the Trp-heme relationships or to the redistribution of molecular species emitting the respective lifetimes. The different lifetimes have been assigned to the native conformation of the Mb with normally oriented heme which possibly corresponds to the τ_1 value. The decay times corresponding to τ_2 could arise from the disordered hemes. The third conformation is the reversibly dissociated heme free Mb whose lifetime is about 4 ns and which corresponds to the interactions of one isomeric form of the hydrated protein with another isomer. Protein surfaces are known to extend the range of their influence via their hydration shells.[22]

Thus, these water-mediated interactions may be optimal when they involve two oppositely charged groups, such as an

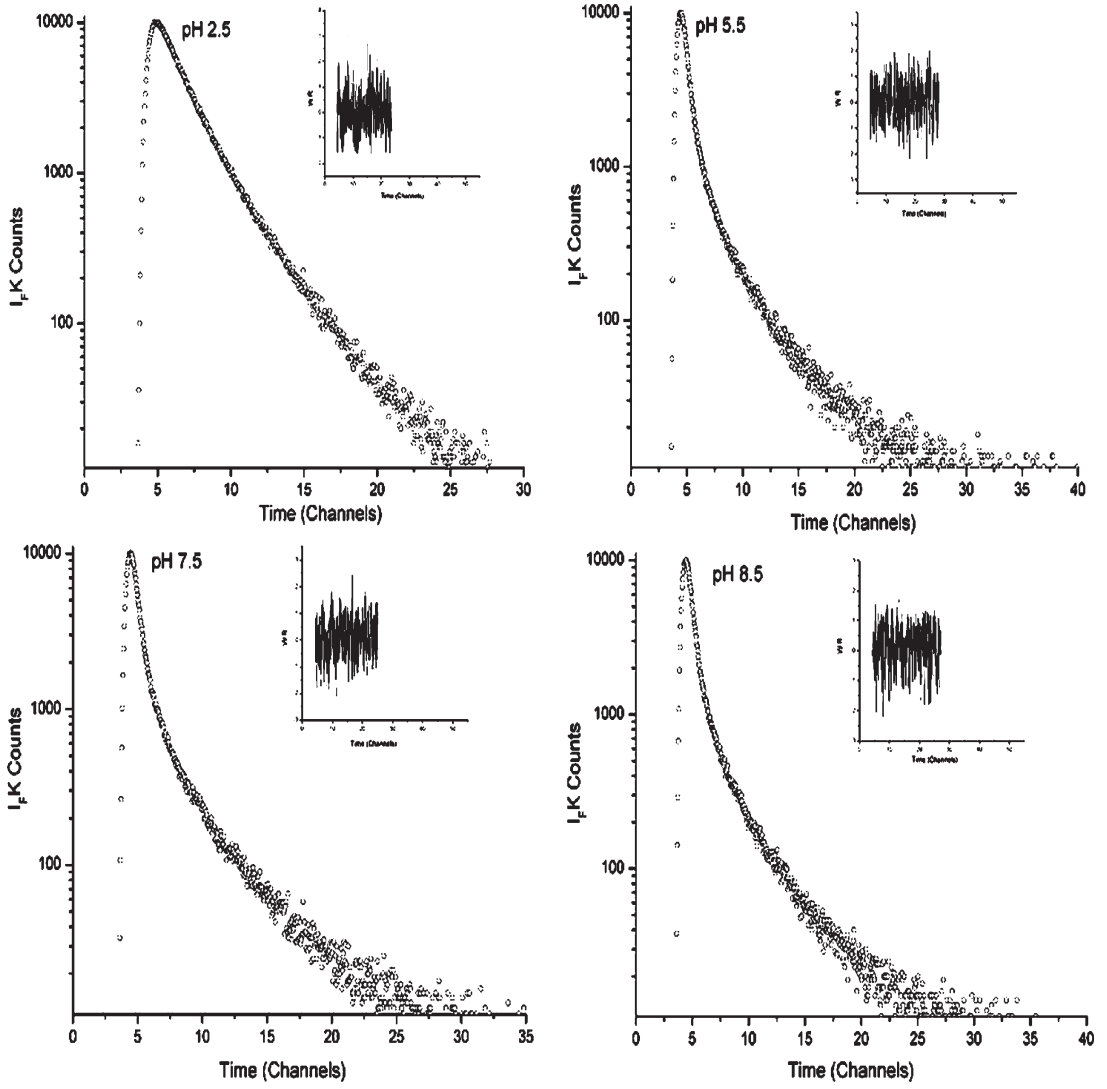

Figure 2. Time-resolved fluorescence decay plots of Mb films (skimmed from air/solution interface after equilibrium) at different pH values.

Table 2. Decay Times of Mb at Different pH

Mb/pH	τ_1 (ns)	% population	τ_2 (ns)	% population	τ_3 (ns)	% population
2.5	1.15 ± 0.03	42.35	2.86 ± 0.02	57.65		
5.5	0.19 ± 0.01	66.97	1.46 ± 0.09	16.05	4.13 ± 0.01	16.98
7.5	0.17 ± 0.001	63.98	1.49 ± 0.01	17.96	4.41 ± 0.12	18.06
8.5	0.19 ± 0.01	65.06	1.59 ± 0.09	18.18	4.39 ± 0.11	16.76

acid−base pair, where the apparently favorable Coulombic interaction of a direct contact is offset by a large Gibbs energy penalty to the complete desolvation of the charges that would be required to make such a contact.

Figure 3a shows the dilational viscosity and elasticity for the protein samples. The plots show that for pH values of 2.5 and 3.5, the system seems to show a viscoelastic behavior. From pH 5.5, the protein solution shows an inverse relationship between viscosity and elasticity. A correlation between the surface tension and the dilational rheological parameters was obtained by studying the relationship between the surface tension and the dilational elastic at different frequencies. Figure 3b presents plots of surface tension versus the rate of change of elasticity. The plots were fitted to a biexponential function represented by eq 1 (Experimental Section).

Table 3 shows the y_0 values, the amplitudes A_1 and A_2, and the times of relaxation t_1 and t_2 for the different Mb samples. It is seen clearly that at pI as expected for best surface coverage, the threshold is the lowest. When a perturbation in the form of dilation of the drop is carried out, the smaller the amplitudes, the faster is the extent of recovery of the surface layer or the system is more elastic. On the basis of this analysis, the system does not exhibit much elasticity below pH 5.5. This is in keeping with the tendency seen in Figure 3a.

dx.doi.org/10.1021/jp2100733 |J. Phys. Chem. B 2012, 116, 895–902

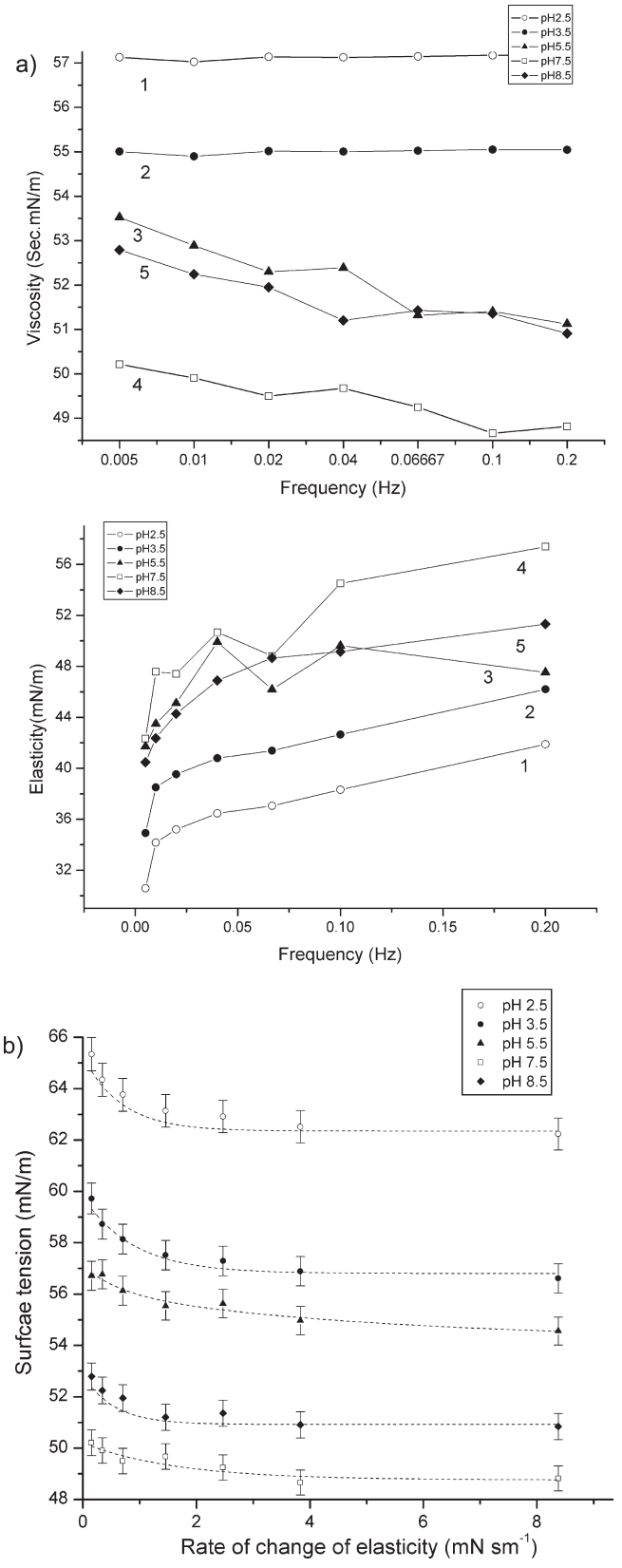

Figure 3. (a) Dilational viscosity and elasticity for the Mb solutions (adsorbed at air/solution interface). (b) Surface tension versus the rate of change of dilational elasticity for the Mb solutions (adsorbed at air/solution interface) (theoretical fit ----).

Table 3. Values of the Amplitudes (A_1, A_2), t_1, t_2, and the y_0 Values for the Different pH Solutions

Mb/pH	y_o	t_1	A_1	t_2	A_2	R^2
2.5	62.19	2.18	2.02	0.18	2.93	0.99
3.5	56.56	0.20	2.99	2.42	2.03	0.99
5.5	53.94	7.42	2.18	0.81	0.97	0.96
7.5	48.70	2.71	0.75	2.71	0.75	0.87
8.5	50.75	0.57	1.65	4.09	0.89	0.96

The dilational rheological parameters deal often with bulk properties. To understand the influence of interactions between the different Mb molecules with themselves and at the interface between solvent molecules at the various pH values, shear rheological studies were undertaken and shear viscosity and shear elasticity were measured. Figure 4a and b represents the shear rheological parameters as a function of time of aging. At pH = 2.5, the adsorbed protein film shows a gradual change in both viscosity and elasticity. The rate of change in the interfacial shear rheological properties is high at pH 7.5 compared with the other pH values. In general, the initial increase in the viscosity values followed by a small dip could possibly arise because of the local relaxation and rearrangement of the protein molecules at the interface.

In all the characteristics exhibited by the protein at the air/solution interface, the strength and high directionality (anisotropy) of the intermolecular interactions in water arising from the network of hydrogen (H) bonding and the effectiveness in solvating ionic and dipolar groups of the protein at different pH's have an appreciable contribution from a surface or interface, namely, water/protein, protein−protein, and protein/air phases. These special properties at the interface arise from the asymmetry in forces experienced by the molecules at the interface. This is seen in many time-dependent properties of the protein such as molecular motions and relaxation.

The time scales range from nanosecond (for water and proteins to interact), picosecond (time scales for the dynamics of water molecules), and tens of seconds which deal with the site-selective water clusters that interact with proteins. Thus, the analysis of water−protein interactions depends strongly on the time scales of measurements and observation. In this regard, the time of aging used to study the shear rheological properties of Mb at the interface is highly relevant. In this study, the changes in shear rheological parameters as a function of aging time have been analyzed using Boussinesq's number.

A linear relationship between shear viscosity and shear rate was first proposed by Boussinesq[49] which is termed the Boussinesq's number. This number is presently used to differentiate between interfacial and bulk processes that influence the rheological parameters. The number is defined as

$$B_0 = \eta_s/\eta_{bulk} \cdot R \qquad (2)$$

where η_S is the shear viscosity, η_{bulk} corresponds to the bulk value, and R is a characteristic distance of the flow geometry obtained from the shear gap of the rheometer. For values of $B \gg 1$, the interfacial organization is undisturbed by the bulk flow, and for $B \ll 1$, the interfacial flow is influenced strongly by the stresses because of the bulk flow. For intermediate values, the two are coupled.

Figure 5 presents the log plots of B_0 versus shear rates. Here, the shear rate is defined as change in shear rheological property as a function of time of aging. The plots are fitted to an allometric

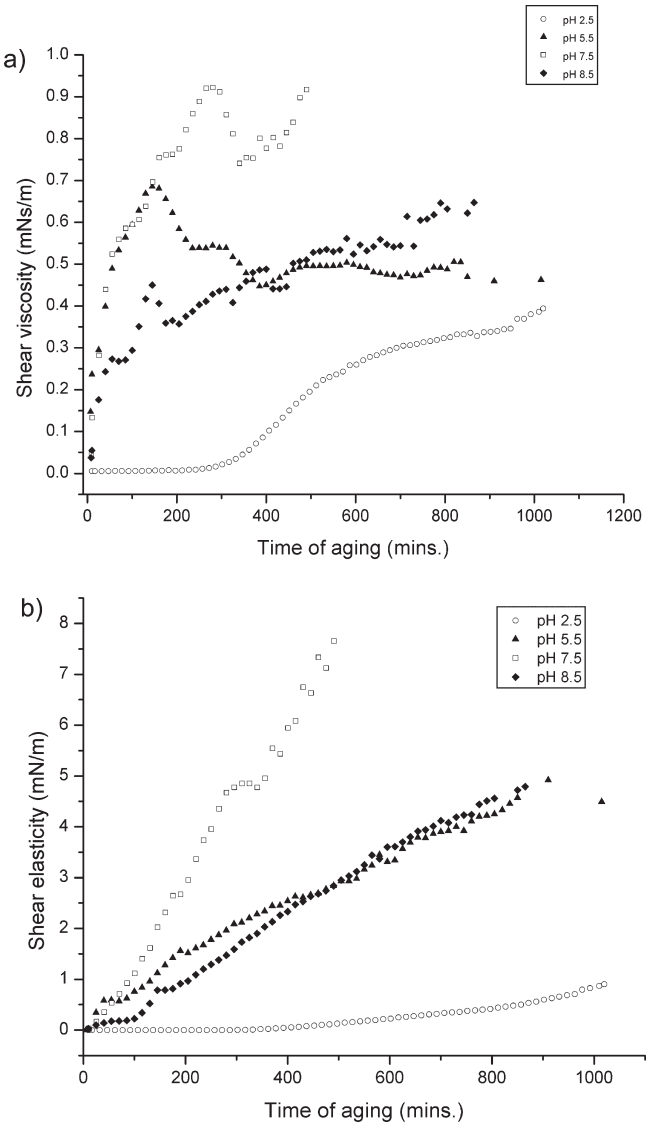

Figure 4. (a) Shear viscosity and (b) elasticity plots of Mb (adsorbed at air/solution interface) at different pH values.

power law function of the form

$$Y = ax^{b} \tag{3}$$

or, for viscosity and shear rate, the equation can be written as

$$\eta = kY^{n-1} \tag{4}$$

where k is the material based constant. Here, the index n defines whether the system is Newtonian or non-Newtonian. For values of $n = 1$, the fluid is Newtonian. For shear thinning, it is between 0 and 1, and for shear thickening, it is greater than 1. Table 4 shows the values of n for the different Mb solutions. The fitted lines are shown as dashed lines.

It is seen that at pH 2.5 the protein behaves like a shear-thickening fluid. At pH 5.5 and 8.5, it is like a shear-thinning fluid or is pseudoplastic. At pI = 7.5, initially the viscosity is independent of shear rate showing a Newtonian behavior. However, after a particular shear rate, there is a drastic reduction or the protein is pseudoplastic. The high extent of pseudoplastic behavior in Mb

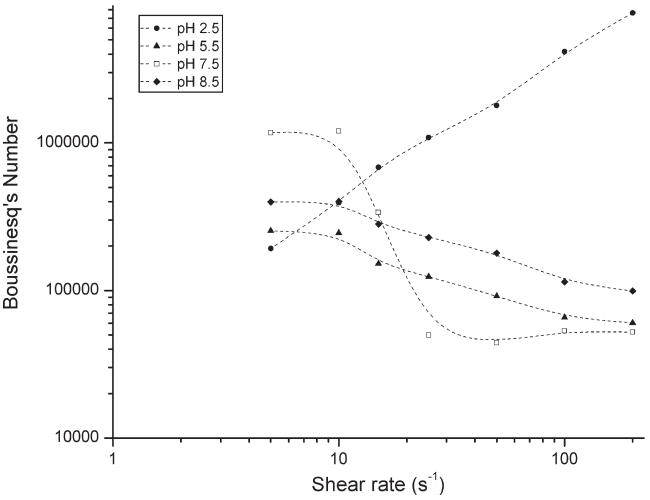

Figure 5. Log plots of Boussinesq's number versus shear rates (theoretical fit ----).

Table 4. Values of n for the Different Mb Solutions

Mb/pH	n
2.5	1.95
5.5	0.56
7.5	0.14
8.5	0.62

at pI indicates an increase in the shear viscosity that could arise from highly cooperative hydrophobic clusters formed because of the change in the pH. These results are strongly suggestive of pH induced formation of hydrophobic clusters. This may appear surprising because the CD spectra of Mb shows a high % of helicity for all pH values above 2.5 showing no drastic changes in the secondary structural features of the protein. However, burial of mainly nonpolar surface area can take place with little change in CD spectrum, and this has been demonstrated in many protein structures.[50−52]

Arunachalam and Gautham have in their review analyzed a large number of protein data sets and have shown that every protein structure consists of at least one large cluster that forms the hydrophobic core and that probably dictates the protein fold and numerous smaller clusters, which might be involved in the stabilization of the fold.[53] Such small clusters could appear at the interface which could then act cooperatively to create a pseudo-plastic fluid at the interface. High surface activity of the protein at pI probably points to the presence of such hydrophobic clusters at the interface.

CONCLUSIONS

On the basis of the results, the observed viscosity reductions at pI can be rationalized in terms of three-dimensional transient protein networks formed in concentrated solutions because of hydrophobic and, to a lesser extent, ionic interactions. It is possible that these reversible protein aggregates are responsible for strong resistance to flow and hence their high viscosity. Future research on flow properties and adsorption of proteins at surfaces should address the dependence of these concepts on the nature of the protein and its size, shape, and hydrophobicity.

dx.doi.org/10.1021/jp2100733 |J. Phys. Chem. B 2012, 116, 895–902

Although the secondary structural features of the protein may vary with the pH of the bulk, the network dynamics of the hydration shell, the overall geometry, and the organization at the interface seem to evolve and to determine the large amplitude protein motions that can result in a viscous drag relative to the bulk. All these factors operating at various time scales determine the overall behavior of the protein at the interface. This study highlights the importance of differentiating the multiple time scales for addressing the complex sequence of events associated with solvation and protein structural transitions and the rheological factors that arise from it.

AUTHOR INFORMATION

Corresponding Author

*E-mail: aruna@clri.res.in. Tel: +91-44-24437167. Fax: +91-44-24911589.

ACKNOWLEDGMENT

The authors would like to thank DST Nanomission for a project grant. The authors would like to acknowledge National Centre for Ultrafast Processes, University of Madras, Chennai, for providing picosecond pump probe spectrometer facility. K.S. would like to thank CSIR, Government of India, for the award of a senior research fellowship.

REFERENCES

(1) Ansari, A.; Jones, C. M.; Henry, E. R.; Hofrichter, J.; Eaton, W. A. *Science* **1992**, *256*, 1796–1798.
(2) Haidekker, M. A.; Ling, T.; Anglo, M.; Stevens, H. Y.; Frangos, J. A.; Theodorakis, E. A. *Chem. Biol.* **2001**, *8*, 123–131.
(3) Craiem, D.; Magin, R. L. *Phys. Biol.* **2010**, *7*, 013001–013003.
(4) Fersht, A. *Structure and Mechanism in Protein Science: A Guide to Enzyme Catalysis and Protein Folding*; W. H. Freeman: New York, 1999.
(5) Auton, M.; Bolen, D. W. *Methods Enzymol.* **2007**, *428*, 397–418.
(6) Pace, C. N. *Methods Enzymol.* **1986**, *131*, 266–280.
(7) Scholtz, J. M.; Barrick, D.; York, E. J.; Steward, J. M.; Baldwin, R. L. *Proc. Natl. Acad. Sci. U.S.A.* **1995**, *92*, 185–189.
(8) Lee, J. C.; Timasheff, S. N. *J. Biol. Chem.* **1981**, *256*, 7193–7201.
(9) Robinson, D. R.; Jencks, W. P. *J. Am. Chem. Soc.* **1965**, *87*, 2462–2469.
(10) Schellman, J. A. *Biophys. J.* **2003**, *85*, 108–125.
(11) Wills, P. R.; Winzor, D. J. *Biopolymers* **1993**, *33*, 1627–1629.
(12) Tanford, C. *Adv. Protein Chem.* **1970**, *24*, 1–95.
(13) Miller, R.; Ferri, J. K.; Javadi, A.; Krägel, J.; Mucic, N.; Wüstneck, R. *Colloid Polym. Sci.* **2010**, *288*, 937–950.
(14) Kotsmar, Cs.; Krägel, J.; Kovalchuk, V. I.; Aksenenko, E. V.; Fainerman, V. B.; Miller, R. *J. Phys. Chem. B* **2009**, *113*, 103–113.
(15) Kazakov, V. N.; Fainerman, V. B.; Kondratenko, P. G.; Elin, A. F.; Sinyachenko, O. V.; Miller, R. *Colloids Surf., B: Biointerfaces* **2008**, *62*, 77–82.
(16) Lakshmanan, M.; Dhathathreyan, A.; Miller, R. *Colloids Surf., A* **2008**, *324*, 194–201.
(17) Muthuselvi, L.; Miller, R.; Dhathathreyan, A. *Chem. Phys. Lett.* **2008**, *465*, 126–130.
(18) Klein-Seetharaman, J.; Oikawa, M.; Grimshaw, S. B.; Wirmer, J.; Duchardt, E.; Ueda, T.; Imoto, T.; Smith, L. J.; Dobson, C. M.; Schwalbe, H. *Science* **2002**, *295*, 1719–1722.
(19) Schuler, B.; Eaton, W. A. *Curr. Opin. Struct. Biol.* **2008**, *18*, 16–26.
(20) Yancey, P. H.; Clark, M. E.; Hand, S. C.; Bowlus, R. D.; Somero, G. N. *Science* **1982**, *217*, 1214–1222.
(21) Agarwal, P. K. *J. Am. Chem. Soc.* **2005**, *127*, 15248–15256.
(22) Swain, J. F.; Gierasch, L. M. *Curr. Opin. Struct. Biol.* **2006**, *16*, 102–108.
(23) Ross, J. *J. Phys. Chem. B* **2006**, *110*, 6987–6990.
(24) O'Brien, E. P.; Ziv, G.; Haran, G.; Brooks, B. R.; Thirumalai, D. *Proc. Natl. Acad. Sci. U.S.A.* **2008**, *36*, 13403–13408.
(25) Sharma, V.; Jaishankar, A.; Wang, Y.-C.; McKinley, G. H. *Soft Matter* **2011**, *7*, 5150.
(26) Stokes, J. R.; Frith, W. J. *Soft Matter* **2008**, *4*, 1133–1140.
(27) Dimitrijev-Dwyer, M.; Middelberg, A. P. J. *Soft Matter* **2011**, *7*, 7772–7781.
(28) Erni, P. *Soft Matter* **2011**, *7*, 7586–7600.
(29) Noskov, B. A.; Grigoriev, D. O.; Latnikova, A. V.; Lin, G.; Loglio, S.-Y.; Miller, R. *J. Phys. Chem. B* **2009**, *113*, 13398–13404.
(30) Xiong, P.; Nocek, J. M.; Griffin, A. K. K.; Wang, J.; Hoffman, B. M. *J. Am. Chem. Soc.* **2009**, *131*, 6938–6939.
(31) Schreiber, G.; Haran, G.; Zhou, H.-X. *Chem. Rev.* **2009**, *109*, 839–860.
(32) Davidson, V. L. *Acc. Chem. Res.* **2008**, *41*, 730–738.
(33) Park, J. D.; Park, J. W. *J. Food Sci.* **2007**, *72*, C202–C207.
(34) Gunda, N. S. K.; Mitra, S. K. *Biomicrofluidics* **2010**, *4*, 014105.
(35) Zhang, Y.; Fujisaki, H.; Straub, J. E. *J. Phys. Chem. B* **2007**, *111*, 3243–3250.
(36) Bellavia, G.; Cottone, G.; Giuffrida, S.; Cupane, A.; Cordone, L. *J. Phys. Chem. B* **2009**, *113*, 11543–11549.
(37) Rector, K. D.; Jiang, J.; Berg, M. A.; Fayer, M. D. *J. Phys. Chem. B* **2001**, *105*, 1081–1092.
(38) Moriyama, Y.; Takeda, K. *J. Phys. Chem. B* **2010**, *114*, 2430–2434.
(39) Finkelstein, I. J.; Massari, A. M.; Fayer, M. D. *Biophys. J.* **2007**, *92*, 3652–3662.
(40) Meng, W.; Raleigh, D. P. *Proteins: Struct., Funct., Bioinf.* **2011**, *79*, 3500–3510.
(41) Loglio, G.; Pandolfini, P.; Miller, R.; Makievski, A. V.; Ravera, F.; Ferrari, M.; Liggieri, L. Drop and bubble shape analysis as tool for dilational rheology studies of interfacial layers. In *Novel Methods to Study Interfacial Layers, Studies in Interface Science*; Möbius, D., Miller, R., Eds.; Elsevier: Amsterdam, 2001; Vol. 11, pp 439−484.
(42) Cicuta, P.; Terentjev, E. M. *Eur. Phys. J. E* **2005**, *16*, 147–158.
(43) Karunakaran, V.; Ramamurthy, P.; Josephrajan, T.; Ramakrishnan, V. T. *Spectrochim. Acta, Part A* **2002**, *58*, 1443–1451.
(44) Whitemore, L.; Wallace, B. *Nucleic Acids Res.* **2004**, *32*, W668–W673.
(45) Krägel, J.; Siegel, S.; Miller, R.; Born, M.; Schano, K.-H. *Colloids Surf., A* **1994**, *91*, 169–180.
(46) Beechem, J. M.; Brand, L. *Annu. Rev. Biochem.* **1985**, *54*, 43–71.
(47) Das, T. K.; Mazumdar, S. *J. Phys. Chem.* **1995**, *99*, 13283–13290.
(48) Gryczynski, Z.; Lubkowski, J.; Bucci, E. *J. Biol. Chem.* **1995**, *270*, 19232–19237.
(49) Boussinesq, M. J. *Ann. Chim. Phys.* **1913**, *29*, 349–357.
(50) Guzman-Casado, M.; Parody-Morreale, A.; Robic, S.; Marqusee, S.; Sanchez-Ruiz, J. M. *J. Mol. Biol.* **2003**, *329*, 731–743.
(51) Carra, J. H.; Anderson, E. A.; Privalov, P. L. *Protein Sci.* **1994**, *3*, 944–951.
(52) Agashe, V. R.; Shastry, M. C. R.; Udgaonkar, J. B. *Nature* **1995**, *377*, 754–757.
(53) Arunachalam, J.; Gautham, N. *Proteins* **2008**, *71*, 2012–2025.